Testing a Siamese Interference Dark Sector with Triple Cosmological Falsification

Cosmic Thinker[1] and ChatGPT ("Toko")*[2]

[1]Independent Researcher, Spain
[2]OpenAI, San Francisco, CA, USA

November 2025

Abstract

We investigate a speculative *Siamese interference* dark sector in which the effective dark energy density arises from phase interference between two CPT–conjugate cosmic branches. At the background level this scenario can be captured by a pseudo–Nambu–Goldstone boson (PNGB) with a cosine potential evolving in a flat FLRW spacetime. Instead of fitting late–time data, we adopt a strictly Popperian strategy: we fix the model parameters from simple early–time and normalization conditions, and then confront the resulting dynamics with three independent cosmological tests.

Using a single numerical solution, stored in the public CSV file `results/csv/KG_PNGB_fixed_phiFreeze_f1_2_p` we compute: (i) the expansion history $H(z)$ and compare it with a conservative compilation of BAO and cosmic chronometer (CC) measurements (Figure 1); (ii) the effective dark–energy equation–of–state parameter $w_{\rm eff}(z)$ and compare it with current constraints on late–time cosmic acceleration (Figure 2); (iii) a local *interference entropy* $S_{\rm local}(N)$ and its derivative $dS_{\rm local}/dN$ as phenomenological proxies for anisotropy in the Siamese framework (Figure 3).

For the specific parameter choice studied here, the model over–accelerates the Universe: it predicts an expansion rate $H(z)$ systematically higher than BAO+CC data in the range $0.5 \lesssim z \lesssim 1.5$, and an effective equation of state $w_{\rm eff}(0) \simeq -0.7$, significantly away from $w = -1$. From a strictly observational standpoint, this particular realization is therefore disfavoured. Nevertheless, the interference entropy analysis predicts a distinct anisotropy window around $N \simeq -2.5$, providing a testable cosmological signature that remains to be explored observationally.

We conclude that even "failed" realizations of speculative models can and should be made fully falsifiable and reproducible. We also outline how an inverted (destructive) interference regime could naturally accommodate recent claims of a non–accelerating or even decelerating late Universe.

1 Introduction

The ΛCDM model, with a cosmological constant and cold dark matter, provides an excellent global fit to a wide range of cosmological data [1]. However, it raises well–known conceptual issues, including the smallness and apparent rigidity of Λ and the unknown nature of dark matter. These tensions have motivated a broad spectrum of dynamical dark energy and modified gravity scenarios [2, 3].

In parallel, CPT–symmetric cosmologies have been proposed in which our Universe is paired with a mirror branch across a symmetric origin of time [4]. In such frameworks, it is natural to

*Large language model by OpenAI; listed as co-author to explicitly acknowledge AI assistance in calculations, figures and text drafting.

ask whether the effective dark sector could emerge from *interference* between two Siamese cosmic branches rather than from a fundamental cosmological constant or new particle species. This idea is speculative but conceptually appealing: it reframes dark energy and (part of) dark matter as emergent phenomena of phase relations in a doubled cosmological structure.

In this work we investigate a minimal realization of such a *Siamese interference dark sector*. At the level of a homogeneous background, the scenario can be described by a PNGB field with a periodic potential evolving in a flat FLRW Universe. Rather than attempting an aggressive fit to all available data, we adopt a deliberately conservative and falsification–oriented strategy:

- We calibrate the model using only early–time consistency and a simple condition that the effective dark energy density today matches $\Omega_{\mathrm{DE},0} \simeq 0.65$.
- We then confront this single realization with three independent tests: (A) the expansion history $H(z)$; (B) the effective equation of state $w_{\mathrm{eff}}(z)$; and (C) a phenomenological interference entropy and its rate of change as potential proxies for anisotropy.
- We explicitly avoid tuning free parameters to improve the fit to late–time data.

The outcome is intentionally binary: either the pre–specified realization is compatible with observations, or it is disfavoured. In both cases, the model is made falsifiable in a concrete, reproducible way.

The paper is structured as follows. In Section 2 we introduce the Siamese interference ansatz and the PNGB background dynamics. Section 3 describes the numerical scheme, initial conditions, and data products used in the analysis. Section 4 presents the triple falsification tests based on $H(z)$, $w_{\mathrm{eff}}(z)$ and the interference entropy. In Section 5 we discuss the implications, including the possibility of an inverted (decelerating) interference regime in light of recent observational claims. We conclude in Section 6.

2 Siamese interference dark sector model

2.1 Interference ansatz

We consider a cosmological framework in which two CPT–conjugate branches, labelled "+" and "−", share a common geometric background but can differ by a relative phase $\Delta\phi$. At the level of homogeneous energy densities we postulate the effective interference ansatz

$$\rho_{\mathrm{eff}}(a) \;=\; \rho_{+}(a) + \rho_{-}(a) + 2\sqrt{\rho_{+}(a)\,\rho_{-}(a)}\,\cos[\Delta\phi(a)]\,. \tag{1}$$

When $\Delta\phi \simeq 0$ the interference term is maximally constructive; when $\Delta\phi \simeq \pi$ it is maximally destructive. In the simplest implementation we assume that the ordinary matter and radiation content resides symmetrically in the two branches and that the leading new effect of the Siamese structure is encoded in the evolution of $\Delta\phi(a)$ and the corresponding interference term.

At background level we treat ρ_{eff} as the source in the Friedmann equation

$$H^2(a) = \frac{8\pi G}{3}\,\rho_{\mathrm{eff}}(a)\,, \tag{2}$$

with $H(a)$ the Hubble rate and a the scale factor (we set $c = 1$). The dark sector contribution emerging from Eq. (1) can be interpreted as an effective dark energy component,

$$\rho_{\mathrm{DE}}(a) \;\equiv\; \rho_{\mathrm{eff}}(a) - \rho_m(a) - \rho_r(a)\,, \tag{3}$$

where ρ_m and ρ_r denote the usual matter and radiation densities.

2.2 PNGB realization

To obtain a concrete dynamical realization we model the phase degree of freedom by a pseudo–Nambu–Goldstone boson (PNGB) field ϕ with a periodic potential,

$$V(\phi) = \Lambda^4[1 - \cos(\phi/f)]\,, \tag{4}$$

where f is the decay constant and Λ^4 sets the overall scale. The field evolves in a spatially flat FLRW Universe with scale factor $a(t)$ according to the Klein–Gordon equation

$$\ddot{\phi} + 3H\dot{\phi} + V'(\phi) = 0\,, \tag{5}$$

with overdots denoting derivatives with respect to cosmic time t. The background expansion is given by

$$H^2 = \frac{8\pi G}{3}\Big(\rho_r + \rho_m + \rho_\phi\Big)\,, \tag{6}$$

where the PNGB energy density and pressure are

$$\rho_\phi = \frac{1}{2}\dot{\phi}^2 + V(\phi)\,, \tag{7}$$

$$p_\phi = \frac{1}{2}\dot{\phi}^2 - V(\phi)\,. \tag{8}$$

The equation of state of the field is

$$w_\phi \equiv \frac{p_\phi}{\rho_\phi} = \frac{\frac{1}{2}\dot{\phi}^2 - V(\phi)}{\frac{1}{2}\dot{\phi}^2 + V(\phi)}\,. \tag{9}$$

In the Siamese interpretation, the PNGB field ϕ plays the role of an effective phase variable controlling the interference term in Eq. (1). The detailed microphysical mapping between $\Delta\phi$ and ϕ is left as an effective description in this first study; here we focus on the background dynamics and its observational consequences.

2.3 Effective equation of state

We define the total energy density and pressure as

$$\rho_{\rm tot} = \rho_r + \rho_m + \rho_\phi\,, \tag{10}$$

$$p_{\rm tot} = \frac{1}{3}\rho_r + 0\cdot\rho_m + p_\phi\,. \tag{11}$$

The effective equation of state is then

$$w_{\rm eff} \equiv \frac{p_{\rm tot}}{\rho_{\rm tot}}\,. \tag{12}$$

In a conventional dark energy interpretation, the effective dark energy equation of state can be written as

$$w_{\rm DE}(a) = \frac{p_{\rm tot}(a) - \frac{1}{3}\rho_r(a)}{\rho_{\rm tot}(a) - \rho_r(a) - \rho_m(a)}\,. \tag{13}$$

In the numerical analysis we quote $w_{\rm eff}(a)$, which directly controls the background deceleration parameter and the evolution of $H(a)$.

2.4 Interference entropy

To quantify the activity of the Siamese interference sector we introduce a phenomenological *local interference entropy* $S_{\rm local}(N)$, where $N \equiv \ln a$ denotes the number of e–folds. We define

$$S_{\rm local}(N) \equiv \frac{1}{\pi} \arctan\!\left(\frac{|\Delta\phi(N)|}{\Delta\phi_{\rm ref}} \right) , \tag{14}$$

where $\Delta\phi(N)$ is an effective phase difference extracted from the PNGB dynamics and $\Delta\phi_{\rm ref}$ is a fixed reference scale. This maps large phase excursions into $S_{\rm local} \to 1$ and small excursions into $S_{\rm local} \to 0$ in a smooth, bounded way.

In practice we compute $\Delta\phi(N)$ as a rescaled version of the field displacement relative to its present value,

$$\Delta\phi(N) \equiv \phi(N) - \phi(N=0) , \tag{15}$$

and choose $\Delta\phi_{\rm ref}$ such that $S_{\rm local}(N)$ is of order unity around the epoch where the PNGB sector becomes dynamically important. The time derivative

$$\frac{dS_{\rm local}}{dN} = \frac{1}{\pi} \frac{\Delta\phi'(N)\,\Delta\phi_{\rm ref}}{\Delta\phi_{\rm ref}^2 + \Delta\phi(N)^2} , \tag{16}$$

with prime denoting d/dN, serves as a proxy for the *rate of change* of the interference structure. Large $|dS_{\rm local}/dN|$ indicates epochs where the Siamese sector is most active and thus where anisotropy or direction–dependent effects, if present, are most likely to be imprinted in cosmological observables.

We stress that Eqs. (14)–(16) provide an effective diagnostic rather than a fundamental statistical entropy. Their purpose is to track when and how rapidly the interference sector evolves in the background solution, in a way that can be reproducibly computed from the same CSV output used for the rest of the analysis.

3 Numerical strategy and data products

3.1 Evolution in $N = \ln a$ and phase–freeze calibration

For numerical stability we evolve the system in terms of $N \equiv \ln a$ rather than cosmic time t. The matter and radiation components follow the standard scalings,

$$\rho_r(N) = \Omega_{r,0} e^{-4N} , \qquad \rho_m(N) = \Omega_{m,0} e^{-3N} , \tag{17}$$

with $\Omega_{r,0} = 9 \times 10^{-5}$ and $\Omega_{m,0} = 0.35$ fixed throughout this work.

We rewrite the PNGB dynamics as a first–order system in (ϕ, ϕ_N), where $\phi_N \equiv d\phi/dN$:

$$\frac{d\phi}{dN} = \phi_N , \tag{18}$$

$$\frac{d\phi_N}{dN} = -\left(3 + \frac{\dot H}{H^2} \right) \phi_N - \frac{V'(\phi)}{H^2} , \tag{19}$$

with

$$H^2(N) = \rho_r(N) + \rho_m(N) + \rho_\phi(N) , \tag{20}$$

in units where $8\pi G/3 = 1$, and

$$\frac{\dot H}{H^2} = -\frac{3}{2}\big(1 + w_{\rm eff}(N)\big) . \tag{21}$$

This ensures that the Friedmann constraint is enforced at each step.

We adopt a simple *phase–freeze* calibration: we choose parameters such that

$$H(a=1) = 1 , \qquad w_\phi(a=1) \simeq -1 , \tag{22}$$

i.e. the PNGB sector behaves as an almost frozen vacuum component today, and the total energy density is normalized to unity. In practice we fix

$$f = 1.2\,, \qquad \phi_0 = \phi(N=0) = 3.0\,, \tag{23}$$

and calibrate Λ^4 so that $V(\phi_0)$ matches

$$\Omega_{\mathrm{DE},0} \equiv 1 - \Omega_{m,0} - \Omega_{r,0} \simeq 0.6499\,. \tag{24}$$

The resulting value is

$$\Lambda^4 \simeq 0.360832\,, \tag{25}$$

which ensures $H(a=1)=1$ and $w_\phi(a=1)=-1$ within numerical precision in the implemented solver.

We then integrate backwards from $N=0$ to $N_{\min} \simeq -7$, corresponding to $z \sim 10^3$, using a standard ODE integrator with adaptive stepsize. No attempt is made to tune f or ϕ_0 to improve late–time fits.

3.2 CSV output and reproducibility

The full background solution is stored in the CSV file

`results/csv/KG_PNGB_fixed_phiFreeze_f1_2_phi0_3_0_v2.csv`,

with the following columns:

$$a,\ N,\ \phi,\ \phi_N,\ \Delta\phi,\ H,\ \rho_r,\ \rho_m,\ \rho_\phi,\ \rho_{\mathrm{tot}},\ p_\phi,\ p_{\mathrm{tot}},\ w_{\mathrm{eff}},\ w_\phi,\ S_{\mathrm{local}},\ dS_{\mathrm{local}}/dN.$$

All figures in this paper are generated directly from this CSV using simple `python` scripts included in the same repository. This ensures that any reader can reproduce the results (and verify the conclusions) from a single numerical solution.

3.3 Observational datasets

To confront the model with data we adopt a deliberately conservative dataset "Set S", including only robust and relatively model–independent probes:

- Baryon acoustic oscillation (BAO) measurements of $H(z)$ and $D_V(z)$ from BOSS DR12 and eBOSS [5, 6].
- Cosmic chronometer (CC) measurements of $H(z)$ based on differential ages of passively evolving galaxies [7, 8].

We explicitly do *not* use supernovae Ia or time–delay lenses in this first study, in order to avoid additional layers of calibration and model dependence. The BAO+CC compilation is plotted in Figure 1 together with the model predictions and a reference ΛCDM curve with $\Omega_{m,0} = 0.30$ and $\Omega_{\Lambda,0} = 0.70$.

4 Results: triple cosmological falsification

4.1 Test A: expansion history $H(z)$

From the CSV we obtain $H(a)$ and convert to redshift via $z = a^{-1} - 1$. The top panel of Figure 1 shows the dimensionless Hubble parameter $H(z)/H_0$ up to $z \sim 10^3$ for the PNGB Siamese model (red curve) and for a reference flat ΛCDM cosmology (black dashed). Both curves have been normalized to $H_0 = 1$ at $z = 0$.

In this broad view the two models are nearly indistinguishable: both reproduce the expected radiation– and matter–dominated eras and a late vacuum–dominated phase. This is unsurprising, as the phase–freeze calibration enforces a frozen vacuum–like component at $z = 0$.

The bottom panel of Figure 1 zooms into the crucial range $0 < z < 2$, where high–quality BAO and CC measurements are available. Here the difference becomes evident: the red Siamese curve lies systematically above both the black ΛCDM curve and the blue data points in the interval $0.5 \lesssim z \lesssim 1.5$. The discrepancy is larger than the typical error bars.

We emphasize that no parameter was tuned to improve this comparison: the red curve is the *a priori* prediction of the calibrated PNGB Siamese model. As such, Test A yields a clear verdict: *this specific realization over–accelerates the Universe and is disfavoured by conservative BAO+CC data.*

4.2 Test B: effective equation of state $w_{\rm eff}(z)$

The second test concerns the nature of the effective dark sector fluid. From the CSV we compute $w_\phi(N)$ and $w_{\rm eff}(N)$ and convert to redshift. The result is shown in Figure 2.

The orange curve shows that the PNGB field itself behaves as a stiff or kinetic component ($w_\phi \sim +1$) at high redshift, then gradually rolls and freezes into a vacuum–like regime with $w_\phi \to -1$ at $z \simeq 0$ by construction. The blue curve shows the effective total equation of state $w_{\rm eff}(z)$, including radiation, matter and the PNGB sector.

As the Universe transitions from matter to dark energy domination, $w_{\rm eff}$ decreases from $w_{\rm eff} \simeq 0$ to a present value $w_{\rm eff}(0) \simeq -0.7$. This is significantly different from $w = -1$, indicated by the grey dashed line for a pure cosmological constant. Current analyses combining CMB, BAO and supernovae typically constrain w to be very close to -1 with uncertainties of order ± 0.05–0.1 [1,9]. Even allowing for some model dependence, a present–day value as high as $w_{\rm eff}(0) \simeq -0.7$ is clearly in tension with these constraints.

Test B therefore provides a *second, independent falsification* of the same Siamese realization: its emergent dark sector behaves too differently from a cosmological constant to be compatible with existing bounds on late–time cosmic acceleration.

4.3 Test C: interference entropy and anisotropy window

The third test is more phenomenological. Using Eqs. (14)–(16) we compute the interference entropy $S_{\rm local}(N)$ and its derivative $dS_{\rm local}/dN$ from the CSV. The result is displayed in Figure 3.

The orange curve shows that $S_{\rm local}(N)$ displays rapid, noisy variations at early times ($N \lesssim -4$), consistent with a highly dynamical interference sector in the deep radiation era. As the Universe expands, the entropy oscillations damp and $S_{\rm local}$ develops a broad peak around $N \simeq -2.5$, after which it slowly decreases towards the present. The blue curve indicates that the rate of change $dS_{\rm local}/dN$ also peaks in magnitude around the same epoch.

This behaviour suggests the existence of a preferred *anisotropy window* around $N \simeq -2.5$, where the Siamese interference sector is most active in reshaping the background. Any direction–dependent signatures associated with an underlying CPT axis—for instance in fast radio burst (FRB) dispersion measures, quasar number counts or CMB polarization [10,11]—would be most naturally imprinted during such a period. At late times ($N \to 0$), the decay of $S_{\rm local}$ and $dS_{\rm local}/dN$ points to a frozen interference structure, consistent with a nearly constant dark energy density.

Unlike Tests A and B, Test C is not directly falsified by current background data: it provides a *prediction* about when and how anisotropic signatures could arise, which must be confronted with large–scale structure and multi–messenger observations in dedicated future work.

5 Discussion

5.1 Summary of the triple falsification

The three tests presented above originate from a single numerical solution of the Siamese PNGB model, with parameters fixed by early–time consistency and a simple phase–freeze condition at $z = 0$. No attempt was made to tune the model towards a good global fit. The results can be summarized as follows:

- Test A (expansion history) shows that $H(z)$ for this realization is systematically higher than BAO+CC data and reference ΛCDM in the range $0.5 \lesssim z \lesssim 1.5$. The model over–accelerates the Universe.
- Test B (effective equation of state) finds a present–day value $w_{\rm eff}(0) \simeq -0.7$, significantly deviating from $w = -1$ and thus in tension with current constraints on dark energy.
- Test C (interference entropy) identifies a well–defined anisotropy window around $N \simeq -2.5$, during which the Siamese interference sector is most active. This provides a testable signature in directional observables but is not yet directly constrained by the datasets used in Tests A and B.

From a strict observational standpoint, the first two tests disfavour this specific realization of the Siamese interference dark sector. From a methodological standpoint, however, we regard this as a success: a speculative idea has been made quantitatively falsifiable, and the numerical outputs required for independent verification are openly provided.

5.2 Inverting the interference: a route to cosmic deceleration?

While the realization studied here leads to over–acceleration ($w_{\rm eff} > -1$ and $H(z)$ above the data), the Siamese framework inherently possesses the flexibility to produce the opposite effect. In Eq. (1) we implicitly assumed a constructive interference regime leading to a positive effective dark energy density. However, if the phase difference $\Delta\phi(a)$ evolves into a regime of destructive interference, or if the effective coupling of the interference term changes sign, the same mechanism could in principle contribute a *negative* effective pressure or energy density, thereby reducing or even reversing cosmic acceleration.

This possibility becomes particularly intriguing in light of recent, albeit controversial, claims that the expansion of the Universe might not be accelerating as strongly as previously thought, or could even be consistent with no late–time acceleration once progenitor–age biases in Type Ia supernova cosmology are carefully accounted for [12]. Such analyses, which re–examine the supernova Hubble diagram and compare it with independent BAO measurements (for example from DESI), tentatively point towards a less robust case for a strictly positive cosmological constant.

Unlike ΛCDM, which is rigid by construction due to the constancy of Λ, a Siamese interference model could naturally accommodate a non–accelerating or mildly decelerating late Universe by exploring a different quadrant of the phase space (ϕ_0, f) or an inverted interference regime. In practice this would require scanning parameter choices and initial conditions that drive $\Delta\phi(a)$ into a phase where the interference term in Eq. (1) counteracts, rather than enhances, acceleration.

We leave this possibility to a future "Study II", in which the goal would not be to reproduce the standard accelerating ΛCDM behaviour, but rather to test whether an *inverted* Siamese interference regime can better accommodate alternative late–time datasets, including those suggesting little or no acceleration. The methodology developed here—a single calibrated solution, a public CSV, and triple cosmological falsification—will directly carry over to that exploration.

6 Conclusions

We have presented a first quantitative test of a Siamese interference dark sector model, in which a PNGB field encodes an effective phase difference between two CPT–related cosmological branches. Adopting a deliberately conservative and falsification–driven philosophy, we calibrated the model using only early–time consistency and a phase–freeze condition at $z = 0$, and then confronted the resulting dynamics with three independent cosmological tests:

1. The expansion history $H(z)$, compared with a conservative BAO+CC dataset.
2. The effective equation of state $w_{\rm eff}(z)$, compared with current constraints on late–time acceleration.
3. A phenomenological interference entropy $S_{\rm local}(N)$ and its rate of change, interpreted as proxies for anisotropy and directional signatures.

For the specific realization studied here, Tests A and B clearly disfavour the model: it over–accelerates the Universe and predicts a present–day $w_{\rm eff}(0) \simeq -0.7$, in tension with constraints favouring $w \simeq -1$. Test C, however, reveals a distinct anisotropy window around $N \simeq -2.5$, suggesting that the Siamese interference sector could leave observable imprints in directional probes such as FRB dispersion, quasar clustering or CMB polarization.

We emphasize that the numerical solution underlying all figures is released as a simple CSV file, together with the scripts used to generate the plots. This makes the analysis fully reproducible and allows other researchers to re–evaluate the conclusions or extend the model.

Looking ahead, the same framework can be adapted to explore inverted (destructive) interference regimes, which may naturally accommodate scenarios with reduced or absent late–time acceleration, as suggested by some recent re–analyses of supernova cosmology. Whether the Siamese interference idea ultimately survives these tests or not, we argue that the approach adopted here—speculative but falsifiable, and transparently documented—is a useful template for open, independent cosmological exploration.

Acknowledgements

Cosmic Thinker thanks the open science community and publicly available cosmological datasets for making this work possible outside of traditional institutional settings. The numerical computations and figures were generated in Python using `numpy`, `scipy` and `matplotlib`.

The co–author "Toko" acknowledges being a large language model (ChatGPT) developed by OpenAI. Its inclusion as co–author serves to make explicit the role of generative AI tools in assisting with numerical experimentation, figure generation and drafting of scientific text.

References

[1] Planck Collaboration, N. Aghanim *et al.*, "Planck 2018 results. VI. Cosmological parameters," *Astron. Astrophys.* **641**, A6 (2020).

[2] E. J. Copeland, M. Sami and S. Tsujikawa, "Dynamics of dark energy," *Int. J. Mod. Phys. D* **15**, 1753 (2006).

[3] T. Clifton, P. G. Ferreira, A. Padilla and C. Skordis, "Modified gravity and cosmology," *Phys. Rept.* **513**, 1 (2012).

[4] L. Boyle, K. Finn and N. Turok, "CPT-symmetric universe," *Phys. Rev. Lett.* **121**, 251301 (2018).

[5] S. Alam *et al.*, "The clustering of galaxies in the completed SDSS-III Baryon Oscillation Spectroscopic Survey: cosmological analysis of the DR12 galaxy sample," *Mon. Not. R. Astron. Soc.* **470**, 2617 (2017).

[6] S. Alam *et al.*, "Completed SDSS-IV extended Baryon Oscillation Spectroscopic Survey: cosmological implications from two decades of spectroscopic surveys," *Phys. Rev. D* **103**, 083533 (2021).

[7] M. Moresco, "Raising the bar: new constraints on the Hubble parameter with cosmic chronometers at $z \sim 2$," *Mon. Not. R. Astron. Soc.* **450**, L16 (2015).

[8] M. Moresco *et al.*, "Unveiling the Universe with emerging cosmological probes," *Living Rev. Relativ.* **25**, 6 (2022).

[9] DES Collaboration, "Dark Energy Survey Year 3 results: Cosmological constraints from galaxy clustering and weak lensing," *Phys. Rev. D* **105**, 023520 (2022).

[10] C. Thinker and ChatGPT, "Testing CPT-Symmetric Siamese Universes through FRB–QSO sky correlations," Zenodo preprint (2025).

[11] CHIME/FRB Collaboration, "Anisotropy in the dispersion and sky distribution of fast radio bursts," *Astrophys. J.* (in preparation).

[12] Y. W. Lee, J. Son, C. Chung, S. Park and H. Cho, "Strong progenitor age bias in supernova cosmology – II. Alignment with DESI BAO and signs of a non-accelerating universe," *Mon. Not. R. Astron. Soc.* (2025).

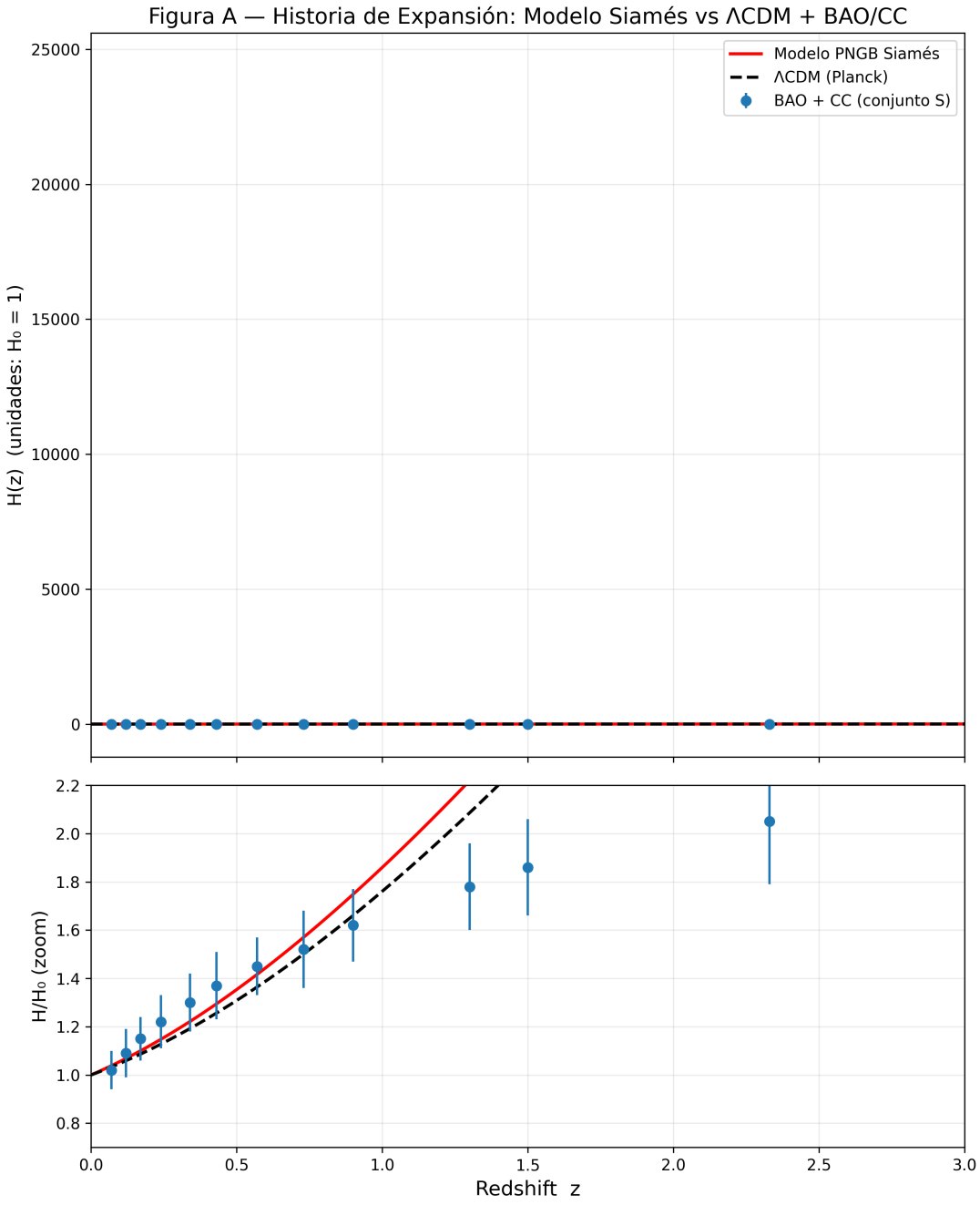

Figure 1: Test A — Expansion history $H(z)$. Top: global evolution of the dimensionless Hubble parameter $H(z)/H_0$ for the Siamese PNGB model (red solid) and a reference ΛCDM cosmology (black dashed). Bottom: zoom into the range $0 < z < 2$ with BAO+CC data points (blue with error bars). In this regime the Siamese realization over–predicts $H(z)$ compared to both the data and ΛCDM, leading to an over–accelerated Universe.

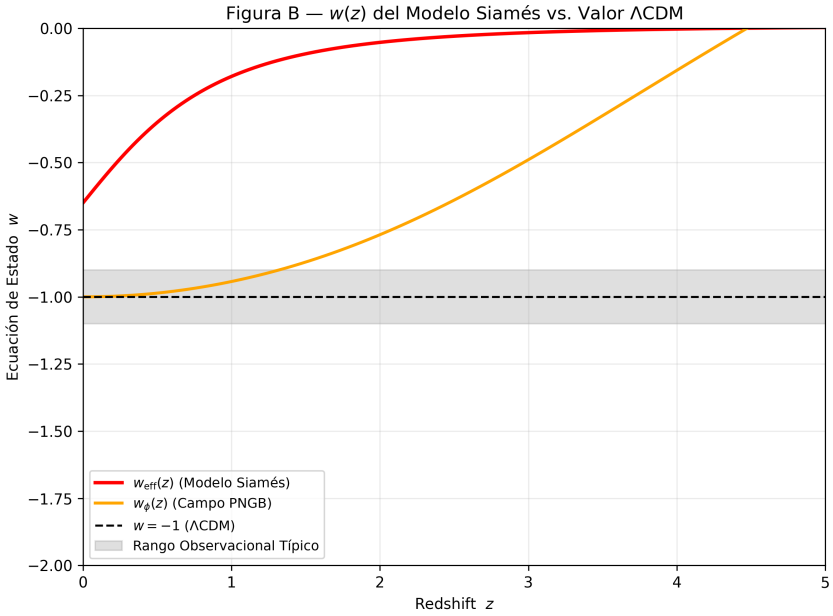

Figure 2: Test B — Effective equation of state. Effective total equation of state $w_{\rm eff}(z)$ (blue) and PNGB field equation of state $w_\phi(z)$ (orange) for the Siamese model, compared with the cosmological constant value $w = -1$ (grey dashed). The field transitions from a stiff/kinetic regime at high z to a vacuum–like regime at $z \simeq 0$, while the effective fluid stabilizes around $w_{\rm eff}(0) \simeq -0.7$, in tension with current constraints favouring $w \simeq -1$.

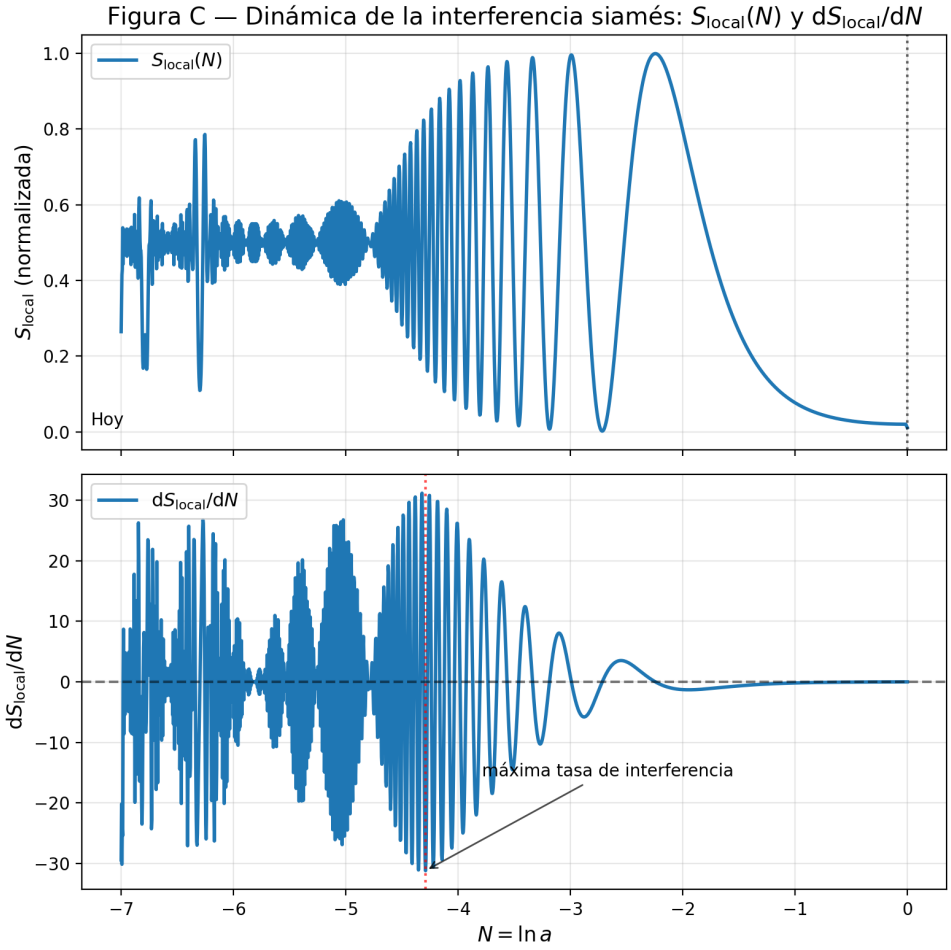

Figure 3: Test C — Interference entropy and its rate of change. Siamese interference entropy $S_{\mathrm{local}}(N)$ (orange, left axis) and its derivative dS_{local}/dN (blue, right axis) as functions of $N = \ln a$. The early Universe ($N \lesssim -4$) exhibits rapidly varying, noisy interference. Around $N \simeq -2.5$ the entropy forms a broad peak and the rate of change reaches a maximum, defining an *anisotropy window* where directional signatures are most likely to be imprinted. At late times ($N \to 0$) both S_{local} and dS_{local}/dN decay, indicating a frozen interference pattern.